PROCEEDINGS OF SCIENCE

Decimation map in 2D for accelerating HMC

Nobuyuki Matsumoto,[a,b,*] **Richard C. Brower**[a] **and Taku Izubuchi**[c,b]

[a] *Boston University, Boston, MA 02215*
[b] *RIKEN/BNL Research Center, Upton, NY 11973, USA*
[c] *Brookhaven National Laboratory, Upton, NY 11973, USA*

E-mail: nmatsum@bu.edu

To accelerate the HMC with field transformation, we consider a variant of the trivializing map, the decimation map, which can be regarded as a coarse-graining transformation. Using the 2D $U(1)$ pure gauge model, combined with the guided Monte Carlo algorithm, we show that the integrated autocorrelation time of the topological charge can be exponentially improved in the wall clock time. Our study indicates that incorporating renormalization group picture is a powerful and essential ingredient to accelerate the HMC at large β.

The 40th International Symposium on Lattice Field Theory (Lattice 2023)
July 31st - August 4th, 2023
Fermi National Accelerator Laboratory

*Speaker

PoS(LATTICE2023)033

1. Introduction

Critical slowing down is intrinsic to Monte Carlo study of lattice quantum field theories, but is not yet resolved satisfactorily. The state of the art algorithm for the gauge field generation in QCD is the Hybrid Monte Carlo (HMC) [1], and there are two major directions to cope with the critical slowing down in this algorithmic framework (see [2, 3] for reviews). One is to align the velocity in the molecular dynamics (MD) among all the Fourier modes [4–8], and the other is to construct a field transformation such that the resulting effective action has advantageous sampling properties [10, 11] (see also [12–18]).

This study follows the latter approach following Lüscher's seminal work [10], and we consider trivialization of link variables. A difference, however, is that we divide the lattice into local blocks while the original work considered the global trivialization. In fact, our field transformation corresponds to eliminating links from the theory, namely *decimation* of the variables. When a link is trivialized, the effective action for the surrounding links exactly agrees with that of the integrated theory. Our approach thus incorporates the idea of renormalization group.

In general, such an algorithm can be extremely complex. We thus first test our idea with the simplest gauge theory possible: the pure $U(1)$ gauge theory in two spacetime dimensions. The peculiarity of this model is that there is no propagation mode; the correlation length defined by the plaquette correlation function is zero. A nontrivial quantity is the topological charge under the periodic boundary condition, which counts the winding number of $U(1)$ plaquette angles around the faces, *i.e.*, the number of vortices. The density of vortices is determined by the susceptibility, which is finite in the continuum limit. In other words, there is a typical volume scale in which a vortex appears. Accordingly, we need to move the variables collectively on fine lattices to induce topological tunneling. In fact, in the HMC, we observe that the tunneling becomes exponentially hard as in QCD. The goal of this study is to demonstrate that the decimation map can reduce the autocorrelation of the topological charge significantly.

The algorithm consists of two parts as in the original trivializing map. We first construct a series of local trivializing maps, namely the *decimation map*, by solving the linear equation for the gradient flow kernel. We here parameterize the function space with Wilson loops and directly invert the linear equation with an iterative solver. We then use the guided Monte Carlo [19] for configuration generation, which is a variant of the HMC replacing the action in the MD Hamiltonian by an approximate one. The effects of finite flow step size and the approximated action are under control and the volume scaling is power-law while keeping the exact detailed balance.

We test our algorithm on a small system of the physical volume $V_{\text{phys}} = 6^2/g^2$, where g is the dimensionful coupling constant. This volume corresponds to the typical scale of a single vortex. We show that we obtain $\times 73$ speedup in the integrated autocorrelation time in wall clock at $\beta = 7.1$ (16×16 lattice), and furthermore, the exponent towards the continuum limit is decreased with a factor of 0.62. Our decimation map exemplifies that the HMC of a gauge theory can be accelerated with a suitable field transformation.

2. Decimation map

The idea of the decimation map can be described simply in the 2D $U(1)$ model with the Wilson action:

$$S(U) \equiv -\beta \sum_x \cos \kappa_x, \tag{1}$$

where $\beta = 1/(ag)^2$ with the lattice spacing a and the coupling g that determines the scale in the system. κ_x is the plaquette angle:

$$\kappa_x \equiv \frac{1}{i} \log(U_{x,0} U_{x+0,1} U^\dagger_{x+1,0} U^\dagger_{x,1}). \tag{2}$$

As in figure 1, we iteratively choose a set of independent link variables to trivialize. Each stage of

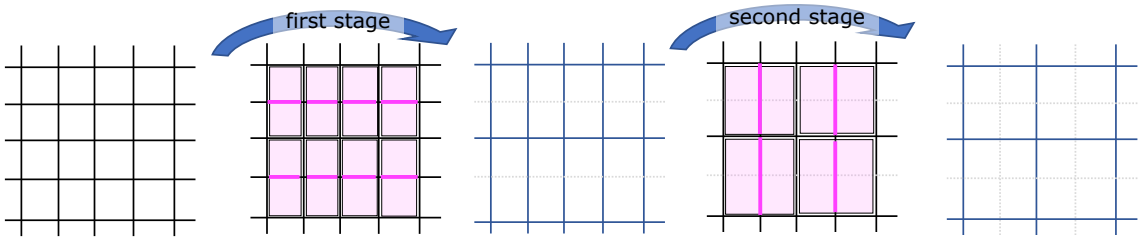

Figure 1: The basic idea of the decimation map is a successive local trivialization of link variables. At each stage, a set of independent link variables (colored with magenta) are chosen and trivialized.

trivialization doubles the size of fundamental Wilson loops in the theory.

Let us write by $U'_{x,\mu}$ the link variables to be trivialized and by $\tilde{U}_{x,\mu}$ the remaining variables. Once the trivialization is performed successfully with the map:

$$U'_{x,\mu} = \mathcal{F}_{x,\mu}(V; \tilde{U}), \tag{3}$$

where $V_{x,\mu}$ are the trivialized variables, the action will be transformed accordingly from the original one $S = S(U', \tilde{U})$ to:

$$S_{\text{eff}}(\tilde{U}) \equiv S(U'(V; \tilde{U}), \tilde{U}) - \ln \det \mathcal{F}^*(V; \tilde{U}), \tag{4}$$

where $\mathcal{F}^*$ is the Jacobian of the map $\mathcal{F}$. Then one can immediately see that S_{eff} agrees with the action we obtain after integrating over U' from the original action:

$$\int (dU')(d\tilde{U}) e^{-S(U', \tilde{U})} = \int (d\tilde{U}) e^{-S_{\text{eff}}(\tilde{U})}. \tag{5}$$

We thus see that $S_{\text{eff}}(\tilde{U})$ describes a coarse-grained system and each stage of the map corresponds to the decimation of links.

Such observation has an important implication that the decimation map drives the system away from the continuum limit, where the HMC becomes inefficient (see figure 2). One can therefore expect that HMC in the decimated system has smaller autocorrelation than in the original system. After obtaining configurations in the decimated system, one can use $\mathcal{F}$ to supply (or *integrate in*) the decimated variables to calculate observables for the original action.

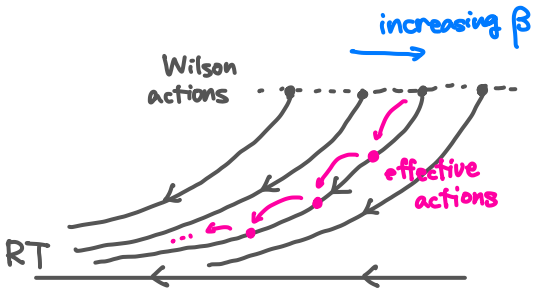

Figure 2: A qualitative picture describing the resulting flow in the action space. It is likely that the theory approaches towards the renormalized trajectory (RT), observing that the tunneling rate is not as high as for the Wilson actions of the larger lattice spacings, at least for the first a few stages. However, it is uncertain how far this picture holds in the flow and its precise structure is out of the scope of this work.

3. Obtaining the map numerically

In our simple example, there are only two Wilson loops attached to each link $U_{x,\mu}$. Let us write by $\kappa_{1,2}$ the two phase angles of the loops. One can take the basis for the function space to trivialize $U_{x,\mu}$ as:

$$e_{m_1,m_2} \equiv \cos(m_1\kappa_1 + m_2\kappa_2) \quad (m_1, m_2 \in \mathbb{Z}). \tag{6}$$

Note that when $m_1 = m_2$, they do not depend on $U_{x,\mu}$, and thus $e_{m,m}$ $(m \in \mathbb{Z})$ are the zero modes of the differential operators.

As in [10], we take the gradient flow ansatz:

$$\dot{U}_{t,x,\mu}U^{-1}_{t,x,\mu} = \partial K_t, \quad U_{t,x,\mu} \equiv \mathcal{F}_{t,x,\mu}(V), \quad \mathcal{F}_{t=1} = \mathcal{F}, \tag{7}$$

where ∂ is the derivative with respect to $\phi \equiv \log U_{x,\mu}$. Then, one can write down the equation for K_t by demanding the effective action to decrease linearly in t. For example, for the first stage:

$$[-\partial^2 + \beta t(\sin\kappa_1 - \sin\kappa_2)\partial]K_t = \beta(\cos\kappa_1 + \cos\kappa_2) + \sum_m e_{m,m}v_{t,m}, \tag{8}$$

For the higher stages, terms with various m_i appear on both hand sides. By representing the differential operator in the basis (6), one can numerically solve the linear equation (8) with, *e.g.*, CGNE with preconditioning by ∂^{-2} in the space without the zero modes. The zero mode part $\sum_m e_{m,m}v_{t,m}$ can be obtained acting the differential operator to the solution after solving the equation in the projected space. We find that for $\beta \lesssim 8.9$, the range $|m_{1,2}| \leq 128$ is sufficient (see figure 5). The inversion takes a few minutes to about a day using GPU depending on the value of β and the stage of decimation. The details of the inversion will be described in the subsequent paper.

In practice, we discretize the flow with the Runge-Kutta methods. We here choose the midpoint integrator. For the map to be bijective, we ensure that the step size is kept within a bound that can be derived as in [10]. For the midpoint integrator, given a kernel of the form:

$$K_t(\phi) = \sum_{m_1,m_2} e_{m_1,m_2}c_{t,m_1,m_2}, \tag{9}$$

the step size ϵ must satisfy:

$$\epsilon B_{t+\epsilon/2} \cdot \left(1 + \frac{\epsilon B_t}{2}\right) < 1, \quad B_t \equiv \sum_{m_1,m_2} (m_1 - m_2)^2 |c_{t,m_1,m_2}|. \tag{10}$$

4. Guided Monte Carlo

The functions $e_{m,m}$ are the Wilson loops of the double size winding m times. They are independent of $U_{x,\mu}$, but have different dependencies on the surrounding links. They are the basis functions for determining the weights in the transformed system. In fact, the integral of the zero mode over t gives the next effective action:

$$S_{\text{eff}} = \sum_m e_{m,m} \int dt\, v_{t,m}. \tag{11}$$

One can use this knowledge to simplify the force calculation with the help of the guided Monte Carlo algorithm [19] as below.

The key point of the guided Monte Carlo algorithm is that, as far as the time evolution in the HMC is symplectic, the detailed balance is exact. However, since the energy conservation is used to have nonvanishing acceptance in the Metropolis test, it is important that the Hamiltonian associated to the symplectic integrator is close to the exact one.

We replace the action in the MD Hamiltonian by an approximate one to evade the evaluation of the gradient of the Jacobian as well as the force propagation. Since the zero modes $v_{t,m}$ are calculable at each flow time t as a sum of Wilson loops, we can calculate the effective action directly in the loop space using eq. (11). We use the Simpson's formula for approximating the right hand side, which involves only one additional evaluation of K_t at $t = 0$ to those calculated for the midpoint integrator. The difference between this approximate action and the effective action of the discretized flow comes from the error in the midpoint integrator and is $O(\epsilon^2)$, where ϵ is the step size of the flow. Note that, though for a fixed ϵ the acceptance rate becomes exponentially small when enlarging the volume, this effect can be compensated by decreasing the step size ϵ of the trivializing flow just as decreasing the MD step size in the conventional HMC. The cost scaling in enlarging the volume is therefore power law.

We set the approximate effective action in the trivialized region to be constant in the MD, and thus we choose the inner links purely randomly. This corresponds to assigning the zero mass in the MD. Nontrivial updates are performed for the outer remaining links through the Wilson loops in the large unit. In the Metropolis test, however, since the replacement involves discretization error of the flow, we need to include all the updated links in the weight function.

In practice, we choose the step size adaptively by making it proportional to the bijection bound (10) while the overall scaling is determined to keep the acceptance around 0.8. The adaptively chosen step size becomes extremely small at large β, however, for the following two reasons. One is that the number of relevant basis functions grows rapidly as β is increased, which will in turn decrease the bijection bound (10) (see also figure 4 on this rapid growth). The other is to control the acceptance rate in the guided Monte Carlo for increasing the lattice sites. In our calculation, the second point is the bottleneck. This cost due to the latter point may be circumvented by using

a higher-order integrator or by switching to calculating the exact force of the effective action as in [10]. As will be shown in section 5, the exponent of the cost towards the continuum limit can be decreased with the decimation map, and thus one can expect an acceleration with the latter algorithm. However, this point needs to be verified with an additional study.

The separation of the inner and outer links corresponds to separating the UV and IR modes in the system. For simplicity, suppose that the decimation map is obtained without discretization error. One can then choose the inner links without autocorrelation. However, since the environmental outer variables are fixed, this fluctuation is only around a fixed background configuration and depends only on the local links surrounding the trivialized region. It can be thus interpreted as the UV fluctuation. On the other hand, the update of the outer links is completely insensible to the inner links, whose dynamics is determined solely by the coarse-grained action. Thus, the global update of the outer links corresponds to updating the IR modes. By using this separation, we can investigate which part of the algorithm is responsible for accelerating the algorithm.

5. Results

To enumerate the effectiveness of our approach, we calculate the integrated autocorrelation time:

$$\tau_{\rm int}(O) \equiv \frac{1}{2} + \sum_{i\geq 1} \frac{\langle O_0 O_i\rangle}{\langle O_0 O_0\rangle}, \tag{12}$$

where $O_i \equiv O(U_i)$ is the value of the observable O evaluated with the i-th configuration U_i. Our interest is in the topological charge [20, 21]:

$$Q \equiv -\frac{1}{2\pi}\sum_x \kappa_x, \tag{13}$$

which is integer-valued. It is assumed to take the principal branch of the logarithm to evaluate κ_x in eq. (2). One can derive analytically that the susceptibility approaches in the continuum limit to:

$$\chi_Q \equiv \frac{\langle Q^2\rangle}{V_{\rm phys}} \to \frac{g^2}{(2\pi)^2} \quad (a\to 0), \tag{14}$$

which shows that a vortex (an instanton) appears typically in a volume of $(2\pi)^2/g^2$.

We fix the physical volume to $V_{\rm phys} = 6^2/g^2$, which is about the scale of a vortex, and take the continuum limit $a \to 0$ by fixing g. The trajectory length of the MD is fixed to 1.0 in all simulations. In the conventional HMC, the MD step size is scaled such that the acceptance rate is around 0.8. In the guided Hamiltonian simulations, the step size is fixed to 0.05 (*i.e.,* 20 steps); though this is not optimal, this number is not relevant to the actual cost because the algorithmic overhead is in the field transformation part. As mentioned in section 4, flow step size of the decimation map determines the acceptance rate, which is scaled for the acceptance to be around 0.8.

Figure 3 shows the scaling of $\tau_{\rm int}(Q)$ in the units of Monte Carlo steps and wall clock time. The number of stages is taken up to four. The computation is performed on CPU without parallelization. As shown in the left panel, for $\beta = 7.1$ (16×16 lattice), $\tau_{\rm int}(Q) \simeq 8000$ with the conventional HMC

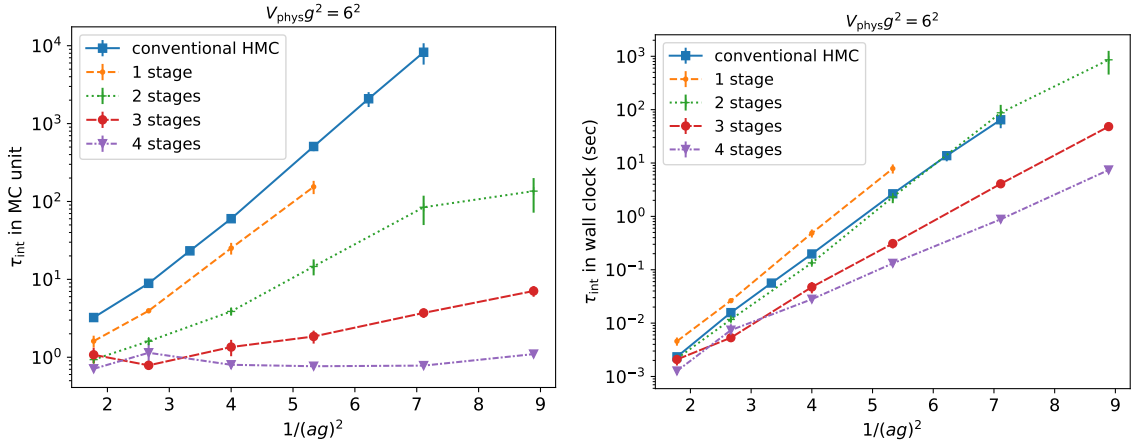

Figure 3: $\tau_{\rm int}(Q)$ in Monte Carlo steps (left) and in wall clock time (right). The conventional HMC (blue solid line) is compared to the guided Monte Carlo with the decimation map up to four stages. In Monte Carlo step, $\tau_{\rm int}(Q) \simeq 8000$ at $\beta = 7.1$ (16×16 lattice) is reduced to $\tau_{\rm int}(Q) \simeq 1$. In wall clock, the speedup at $\beta = 7.1$ is x73 and the decrease of the exponent is by a factor 0.62 with four stages.

is reduced to $\tau_{\rm int}(Q) \simeq 1$ with the decimation map in the Monte Carlo unit. In wall clock, we see x73 speedup at $\beta = 7.1$, and furthermore, the exponent has decreased with a factor of 0.62.

Concerning the algorithmic overhead, it is the second stage of decimation that is the most costly (see figure 4). This is simply because the number of relevant basis functions is the largest. Figure 5

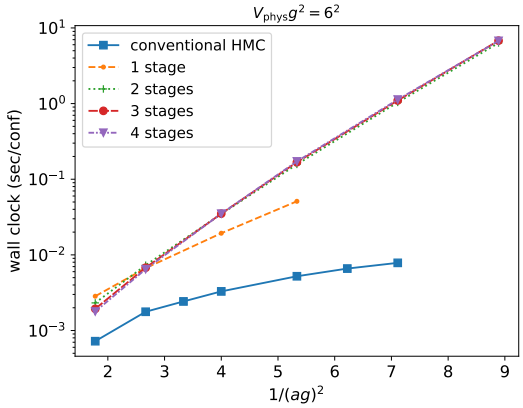

Figure 4: The time consumed to generate a configuration in wall clock. Since the second stage is the most costly, this part dominates the time even when we include higher stages.

shows the magnitude of the coefficients c_{t,m_1,m_2} of eq. (9) for $\beta = 8.9$ at $t = 1$ (corresponding to the finest lattice during the transformation). After the first stage, the functions with large $m_1 - m_2$ become relevant as the effective action contains terms of higher representations, multiply winded loops. At the later stages, the number of relevant basis functions decreases reflecting that the lattice is becoming coarse.

Figure 6 shows the time series of Q at $\beta = 7.1$ with and without the decimation map. With the conventional HMC, we observe that Q is varying extremely slowly in large scale; the fast fluctuation only moves Q back and forth between two nearby sectors. By implementing the decimation map,

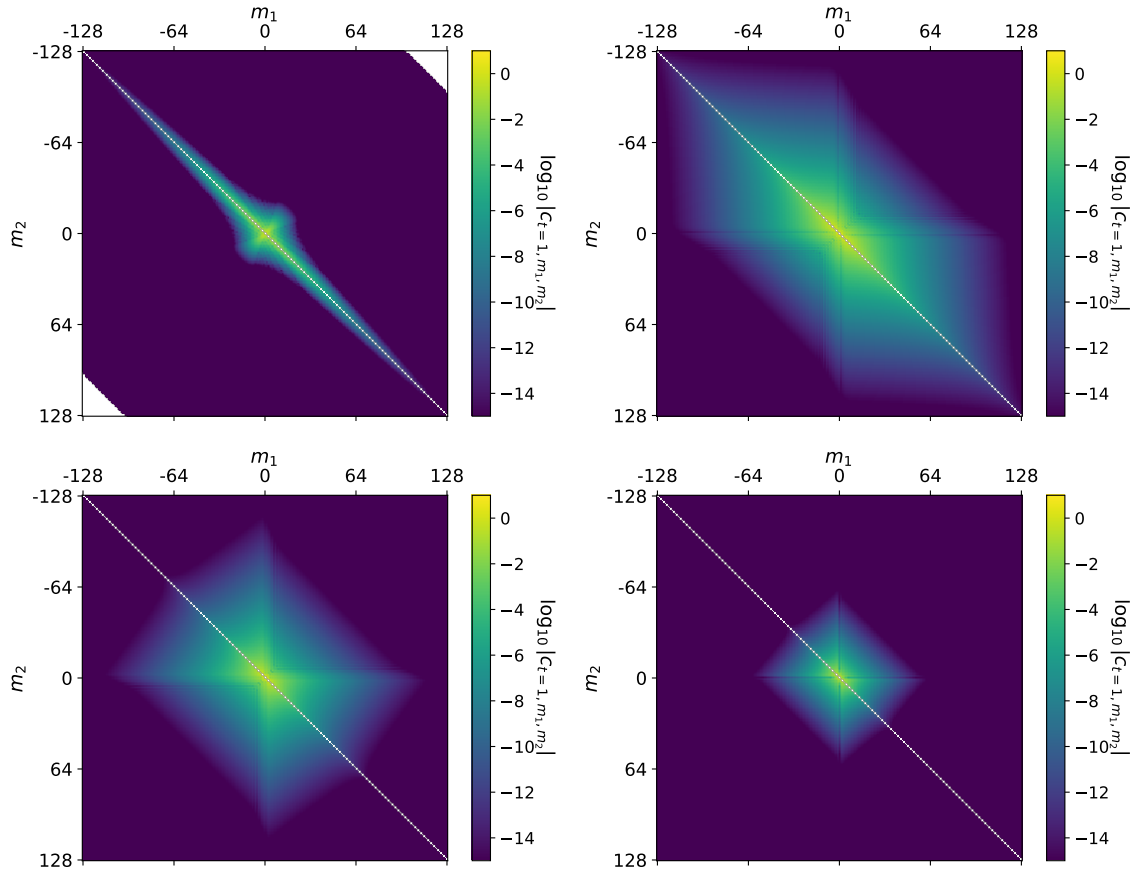

Figure 5: Density plot of the magnitude of the coefficient function in the flow kernel at $t = 1$ (corresponding to the finest lattice during the transformation) for $\beta = 8.9$. The first to fourth stages from top left to right bottom. The relevant basis functions expand in the $m_1 - m_2$ direction after the first stage because the effective action includes multiply winding Wilson loops. After the second stage, the number of relevant functions decreases reflecting that the lattice action is becoming coarse.

the fluctuation becomes centered correctly at $Q = 0$ without visible long-range autocorrelation even though a single update is taking a noticeable time.

Finally, to study whether it is the UV or IR part of the algorithm that is generating the acceleration, we separate the inner (UV) and outer (IR) updates by freezing one of them alternatively, and measure the tunneling rate:

$$R \equiv \langle |Q_i - Q_{i+1}| \rangle. \tag{15}$$

Figure 7 shows R for each part with various β. For small β, the volume of the trivialized region is large enough to create a vortex. Correspondingly, the inner update has a larger tunneling rate compared to the outer update. However, as we enlarge β, the chance of creating a vortex inside the trivialized region becomes small, and the effectiveness flips.

As discussed in section 4, the outer update is necessary to change the global configuration. Consequently, even when the topological charge changes in the UV update, the central value of the fluctuation will not change unless the IR modes are altered. In large β theories, since the problem

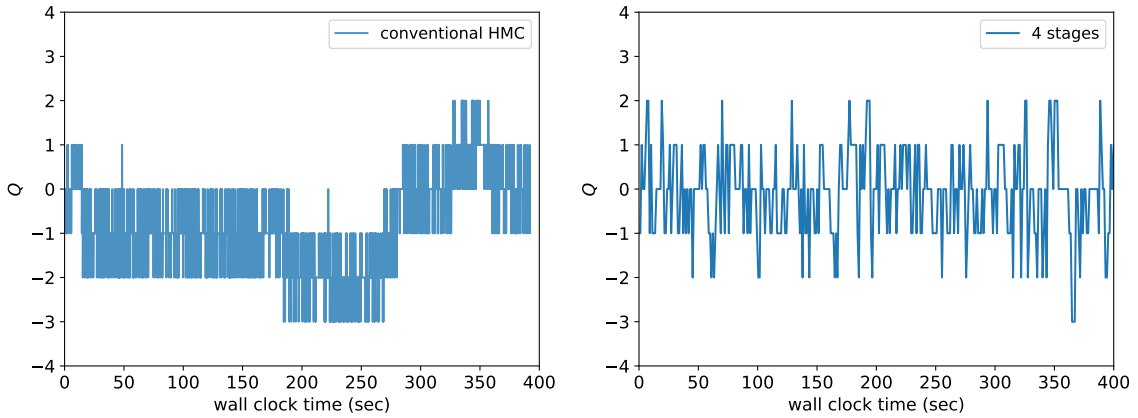

Figure 6: Time series of the topological charge in wall clock with the conventional HMC (left) and with the decimation map with four stages (right) at $\beta = 7.1$. With the conventional HMC, though Q changes back and forth frequently within two nearby sectors, it takes a long time to cover all the topological sectors because of the large autocorrelation. With the decimation map, on the other hand, though each update takes a noticeable time, it spans all the sectors with a few Monte Carlo steps thanks to the minimal autocorrelation.

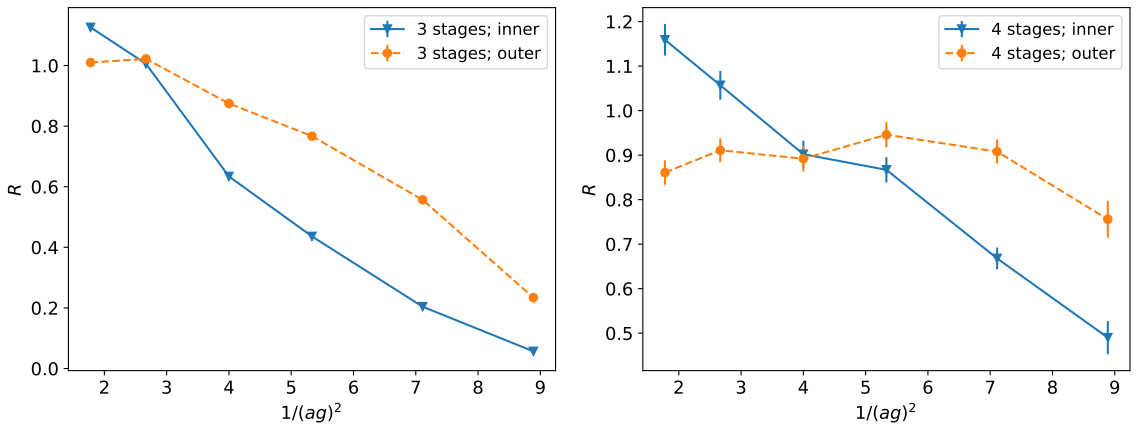

Figure 7: Comparison of the tunneling rate R compared between the inner UV update and the outer IR update with three and four stages of decimation. For small β, since a vortex can fit into a local trivialized region easily, the inner update gives larger R. However, as we increase β, the link variables start to form a continuum, and consequently they need to be updated collectively. Accordingly, the outer IR update becomes more effective at large β.

is to update the IR modes effectively, mapping the theory to coarse lattice actions by incorporating renormalization group seems crucial for the speed up.

6. Conclusion and Outlook

We considered the decimation map in the 2D $U(1)$ model that can be regarded as a coarse-graining transformation. With this map, combined with the guided Monte Carlo algorithm, we showed that the integrated autocorrelation time of the topological charge can be exponentially improved in the wall clock time. We observe x73 speed up on the 16×16 lattice at $\beta = 7.1$ and the

decrease of the exponent by a factor of 0.62. Our study exemplifies that it is possible to accelerate the HMC in gauge theories once an appropriate field transformation is constructed. We further argued that the coarse-graining picture is crucial for accelerating the HMC at large β.

Towards the application in QCD, there are three points to be addressed: generalization to non-Abelian groups, generalization to higher dimensions, and inclusion of the fermion; and none of them is straightforward. However, machinery of solving the linear equation itself can be applied to non-Abelian cases in principle by parameterizing the function space with the Wilson loops. The nontrivial relations among the Wilson loops called Mandelstam constraints [22] (see also [18]) will not be an issue in finding a solution with iterative methods. Generalization to higher dimension needs work even for the $U(1)$ case because the variables correlate through various directions and the effective action involves loops with complicated shapes. Nevertheless, if we can trivialize codimension-one hypersurfaces completely, the resulting effective theory will be described by the double-sized Wilson loops by gauge invariance. However, aiming further to include fermion, it must be necessary to find an approximation scheme rather than solving the equation exactly while retaining the renormalization-group picture. Toy 2D models such as the CP^{N-1} model and the Schwinger model may be useful for such investigations. Studies along these lines are in progress and will be reported elsewhere.

Acknowledgments

The authors thank Tom Blum, Peter Boyle, Norman Christ, Gerald Dunne, Sam Foreman, Anna Hasenfratz, Luchang Jin, Xiaoyong Jin, Chulwoo Jung, James Osborn, Akio Tomiya, Julian Urban and Urs Wenger for valuable discussions. This work is supported by the U.S. Department of Energy under contract No. DE-AC02-07CH11359. N.M. was supported by the Special Postdoctoral Researchers Program of RIKEN.

References

[1] S. Duane, A. D. Kennedy, B. J. Pendleton and D. Roweth, *Hybrid Monte Carlo*, Phys. Lett. B **195**, 216-222 (1987).

[2] G. Kanwar, *Flow-based sampling for lattice field theories*, PoS(LATTICE2023)114.

[3] P. Boyle, *Advances in algorithms for solvers and gauge generation*, PoS(LATTICE2023)122.

[4] G. Parisi, *Prolegomena to Any Future Computer Evaluation of the QCD Mass Spectrum*, Progress in Gauge Field Theory, edited by 't Hooft et al. (Plenum, New York, 1984), p.351.

[5] G. G. Batrouni, G. R. Katz, A. S. Kronfeld, G. P. Lepage, B. Svetitsky and K. G. Wilson, *Langevin Simulations of Lattice Field Theories*, Phys. Rev. D **32**, 2736 (1985).

[6] C. T. H. Davies, G. G. Batrouni, G. R. Katz, A. S. Kronfeld, G. P. Lepage, K. G. Wilson, P. Rossi and B. Svetitsky, *Fourier Acceleration in Lattice Gauge Theories. 1. Landau Gauge Fixing*, Phys. Rev. D **37**, 1581 (1988).

[7] G. Katz, G. Batrouni, C. Davies, A. S. Kronfeld, P. Lepage, P. Rossi, B. Svetitsky and K. Wilson, *Fourier Acceleration. 2. Matrix Inversion and the Quark Propagator*, Phys. Rev. D **37**, 1589 (1988).

[8] C. T. H. Davies, G. G. Batrouni, G. R. Katz, A. S. Kronfeld, G. P. Lepage, P. Rossi, B. Svetitsky and K. G. Wilson, *Fourier Acceleration in Lattice Gauge Theories. 3. Updating Field Configurations*, Phys. Rev. D **41**, 1953 (1990).

[9] T. Nguyen, P. Boyle, N. H. Christ, Y. C. Jang and C. Jung, *Riemannian Manifold Hybrid Monte Carlo in Lattice QCD*, PoS **LATTICE2021**, 582 (2022) [arXiv:2112.04556 [hep-lat]].

[10] M. Luscher, *Trivializing maps, the Wilson flow and the HMC algorithm*, Commun. Math. Phys. **293**, 899-919 (2010) [arXiv:0907.5491 [hep-lat]].

[11] G. P. Engel and S. Schaefer, *Testing trivializing maps in the Hybrid Monte Carlo algorithm*, Comput. Phys. Commun. **182**, 2107-2114 (2011) [arXiv:1102.1852 [hep-lat]].

[12] M. S. Albergo, G. Kanwar and P. E. Shanahan, *Flow-based generative models for Markov chain Monte Carlo in lattice field theory*, Phys. Rev. D **100**, no.3, 034515 (2019) [arXiv:1904.12072 [hep-lat]].

[13] S. Foreman, X. Y. Jin and J. C. Osborn, *Deep Learning Hamiltonian Monte Carlo*, [arXiv:2105.03418 [hep-lat]].

[14] D. Albandea, P. Hernández, A. Ramos and F. Romero-López, *Topological sampling through windings*, Eur. Phys. J. C **81**, no.10, 873 (2021) [arXiv:2106.14234 [hep-lat]].

[15] S. Foreman, T. Izubuchi, L. Jin, X. Y. Jin, J. C. Osborn and A. Tomiya, *HMC with Normalizing Flows*, PoS **LATTICE2021**, 073 (2022) [arXiv:2112.01586 [cs.LG]].

[16] M. Caselle, E. Cellini, A. Nada and M. Panero, *Stochastic normalizing flows as non-equilibrium transformations*, JHEP **07**, 015 (2022) [arXiv:2201.08862 [hep-lat]].

[17] S. Bacchio, P. Kessel, S. Schaefer and L. Vaitl, *Learning trivializing gradient flows for lattice gauge theories*, Phys. Rev. D **107**, no.5, L051504 (2023) [arXiv:2212.08469 [hep-lat]].

[18] P. Boyle, T. Izubuchi, L. Jin, C. Jung, C. Lehner, N. Matsumoto and A. Tomiya, *Use of Schwinger-Dyson equation in constructing an approximate trivializing map*, PoS **LATTICE2022**, 229 (2023) [arXiv:2212.11387 [hep-lat]].

[19] A. M. Horowitz, *A Generalized guided Monte Carlo algorithm*, Phys. Lett. B **268**, 247-252 (1991).

[20] M. Luscher, *Topology of Lattice Gauge Fields*, Commun. Math. Phys. **85**, 39 (1982).

[21] A. Phillips, *Characteristic Numbers of U(1) Valued Lattice Gauge Fields*, Annals Phys. **161**, 399-422 (1985).

[22] S. Mandelstam, *Charge - Monopole Duality and the Phases of Nonabelian Gauge Theories*, Phys. Rev. D **19**, 2391 (1979).